

## **UC Davis**

### **UC Davis Previously Published Works**

#### **Title**

New strategies for resolving oligosaccharide isomers by exploiting mechanistic and thermochemical aspects of fragment ion formation

#### **Permalink**

<https://escholarship.org/uc/item/9s71w96v>

#### **Authors**

Guerrero, Andres  
Lebrilla, Carlito B

#### **Publication Date**

2013-11-01

#### **DOI**

10.1016/j.ijms.2013.05.002

Peer reviewed

Published in final edited form as:

*Int J Mass Spectrom.* 2013 November 15; 354-355: . doi:10.1016/j.ijms.2013.05.002.

## New strategies for resolving oligosaccharide isomers by exploiting mechanistic and thermochemical aspects of fragment ion formation

Andres Guerrero<sup>a</sup> and Carlito B. Lebrilla<sup>a,\*</sup>

<sup>a</sup>Department of Chemistry, University of California Davis, CA 95616, United States

### Abstract

Three complementary experimental approaches for elucidating human milk oligosaccharide (HMOs) isomers by Fourier Transform Ion Cyclotron Resonance mass spectrometry (FT-ICR) are described: tandem-MS disruption by double resonance to distinguish different fragmentation pathways, examination of fragment intensity ratios arising from differential alkali metal ion affinities and monitoring competitive fragmentation rates. The interpretation of the fragmentation pattern from a mechanistic and thermochemical point of view permits the assignment of not only pure isomers but, in some cases, mixtures of them. Methodologically the procedures are simple, reliable and rapid making unnecessary both the use of previous separation techniques and tedious chemical modifications of the HMOs. In principle, the rationale can be expanded to resolve other isomeric mixtures of biological nature.

### Keywords

IRMPD; FT-ICR; Oligosaccharides; Double resonance; Fragmentation pathway; Sodium affinity

## 1. Introduction

Oligosaccharides are very common macromolecules present in nature as glycoconjugates or as free species [1–3]. These compounds can differ in size, monosaccharide composition, sequence, branching, linkage and anomeric configuration [4]. In biological samples, oligosaccharides amounts can also vary across many orders of magnitude. There has been recent significant interest in these compounds led by the increasing realization of their roles in many biological processes [5–7]. For this reason, there has been many new developments in the analysis that have made structure elucidation more facile [8]. However, despite advances in these methods, the analysis of oligosaccharides remains far from routine, and often various structural types require different analytical tools.

Mass spectrometry (MS) has emerged as arguably the most useful method for the structural elucidation of oligosaccharides [9, 10]. Structural elucidation is enabled by tandem MS (MS/MS), perderivatization or enzymatic digestion of native structures [11]. MS/MS techniques have been extensively used for this purpose with variable success [12–18]. Quite

© 2013 Elsevier B.V. All rights reserved

\*Corresponding author cblebrilla@ucdavis.edu.

**Publisher's Disclaimer:** This is a PDF file of an unedited manuscript that has been accepted for publication. As a service to our customers we are providing this early version of the manuscript. The manuscript will undergo copyediting, typesetting, and review of the resulting proof before it is published in its final citable form. Please note that during the production process errors may be discovered which could affect the content, and all legal disclaimers that apply to the journal pertain.

common is the modification of the oligosaccharides by different chemical reactions including permethylation [11, 15], peracetylation [14], reduction [17], periodate oxidation [18] or trifluoroacetylation [16] in order to increase the signal, stabilize the oligosaccharide, eliminate the alditol form or promote a specific fragmentation.

One important biological fluid where oligosaccharides play a role is milk. Free oligosaccharides are a major component of the milk, especially in the human where they can be found in concentrations of 7–12 g/L [19]. It is well-known that human milk oligosaccharides (HMOs) have several beneficial roles during the development of the infant such as providing nutrient for beneficial bacteria [20, 21], prevention of adhesion of the pathogenic bacteria on the intestinal surface [22], immunomodulation [23, 24] and modification of the cell glycome [25]. Positional isomers are also abundant in HMOs and these structural differences have important biological relevance. For example, the linkage pattern of the fucosylated moiety in HMOs defines the antigens Lewis<sup>A</sup> and Lewis<sup>X</sup> that are known to have distinct biological functions in cell-to-cell recognition processes [26, 27].

The intensities of the fragment ions in tandem MS experiments are the result of a complex combination of factors such as the relative stability of precursors and products, bond strengths, activation barriers or position of the charge [28, 29]. All these factors are in turn the consequence of a specific chemical structure. Hence, even when isomers can yield the same products in tandem MS experiments, they may often be resolved by based on the relative abundances of the fragment ions.

In the present study we show the systematic examination of the pathways and product ions generated by infrared multiphoton dissociation (IRMPD) of representative HMOs. The interpretation of the fragmentation pattern observed for these molecules provided an unexpected amount of information concerning its structure and was used not only to distinguish different pure isomers but mixtures of them. Furthermore, the experiments were performed without chemical modification or previous separation of the oligosaccharides what significantly simplified the procedure.

## 2. Experimental Methods

Mass measurements were performed by using a MALDI-FT-ICR (IonSpec, Irvine, CA) instrument equipped with a 7.0-T superconducting magnet. The instrument is equipped with a pulsed Nd:YAG laser (355nm). The details of the instrument are published elsewhere [30]. The instrument was calibrated using a natural mixture of maltooligosaccharides from beer as described in previous publications [31].

The oligosaccharides used in this study include isomers LNFP I, LNFP II, LNFP III and LNFP V, isomers LNDFH I and LNDFH II, and were acquired from Glyko®. The compounds were of analytical grade and were used without further purification. The MALDI matrix 2,5-DHB and NaCl were obtained from Sigma-Aldrich®. The MALDI samples were prepared by applying on the MALDI plate in the following order a 0.5 µL solution of the oligosaccharide (10 µg/mL), 0.5 µL of 2,5-DHB solution (50 µg/mL) and 0.2 µL of NaCl (0.1 M), all in 50:50 AcN/H<sub>2</sub>O. The sample was dried in the vacuum in the pre-chamber of the MALDI source.

The tandem MS IRMPD experiments were performed using a 1060nm instrument (Parallax Tech. Inc.) with varying irradiation times. Double resonance experiments were accomplished by applying a burst excitation pulse to the desired ion during the IRMPD fragmentation. The voltage in each case was optimized to be the minimum necessary to eliminate the desired fragment in order to avoid expulsion of other informative ions.

### 3. Results and Discussion

Three complementary procedures are described illustrating that it is possible to resolve isomers of complicated structures employing only mass spectrometry by taking advantage of both the mechanistic differences in the fragmentation pathways and the thermochemical properties of the molecules. Four isomers of lacto-N-fucopentaose and two of lacto-N-difucohexaose (Scheme 1) from human milk [19] were used to develop and illustrate the methods.

#### 3.1 Distinguishing isomers by disruption of the fragmentation pathways through double resonance

Most methods employed to identify isomers by MS/MS are based on the assignment of product ions after the fragmentation process relying on diagnostic peaks that are unique to specific structures. Unfortunately many isomers do not yield unique fragments and the tandem mass spectra are often indistinguishable. For example, the IRMPD of LNFP I and LNFP II in Figures 1a and 1c, respectively, show the same product ions with nearly the same abundances.

Despite the close similarities in the fragment composition, it is possible to resolve isomers by probing the differential pathways that generate the product ions. Scheme 2 shows the potential fragmentation pathways of isomers LNFP I and LNFP II starting with the sodiated parent. The diagram is based on the product ions formed after IRMPD and shows most of the potential routes that create them. The main difference between the two corresponding tandem MS is the presence of the product ion  $m/z$  714 in LNFP II, which corresponds to the cleavage of the galactose from the branched terminus. Although the presence of this very minor fragment may be sufficient to differentiate the two isomers, it is often found in very low abundances when present and often not at all even for LNFP II.

An examination of Scheme 2 shows a difference between the two isomers for the formation of the ion  $m/z$  568. Two simultaneous pathways generate this product ion in the fragmentation of LNFP I, the stepwise loss of the fucose and the galactose from the non-reducing terminus and the concerted cleavage of the disaccharide from the precursor ion. In the branched isomers LNFP II and LNFP III the latter pathway is not possible. That is, formation of product ion  $m/z$  568 occurs only after the sequential losses of fucose ( $m/z$  730) and galactose or vice versa, loss of galactose ( $m/z$  714) first from the branched terminus (Scheme 2). The pathway was probed in the FT-ICR during tandem MS with IRMPD by employing a double resonance ejection pulse of the intermediate species involved in the formation of product ion  $m/z$  568. The ejection of fragment ions  $m/z$  730 and  $m/z$  714 from LNFP I yields the same abundances of  $m/z$  568 (Figure 1b) confirming the presence of an alternative mechanism to the sequential losses of a fucose and a galactose. However, the ejection of the same two ions from LNFP II during IRMPD eliminates the fragment ion  $m/z$  568 completely suggesting that this product is only produced through those intermediates (Figure 1d).

In general, this method is applicable for differentiating linear and branched structures. Another example is given in Figure 2 with the isomers LNDFH I and LNDFH II. Both LNDFH I and LNDFH II yield essentially the same fragmentation products (Figure 2a and 2c, respectively). As in the previous case, the product ion  $m/z$  568 is generated simultaneously by two fragmentation pathways for the linear isomer LNDFH I, while in the branched one LNDFH II the direct cleavage of the disaccharide to form the same fragment is not possible. Thus, the ejection of the appropriate intermediate product causes the elimination of specie  $m/z$  568 in LNDFH II (Figure 2d) but not in LNDFH I (Figure 2b).

### 3.2 Distinguishing isomers based on differential dopant affinities

In MALDI-MS of oligosaccharides a dopant salt, typically alkali metals such as sodium chloride, are used to produce a single quasimolecular ion corresponding to the coordinated metal [32]. Oligosaccharides ions formed by metal attachment present some advantages for analytical tandem MS over the ionic species generated by proton attachment. For example, some metal-coordinated oligosaccharide ions may give cross-ring products yielding information regarding the linkage [33]. Furthermore, alkali metals stabilize labile residues like sialic acid [34] thereby increasing the sensitivity of the method. For this reason the oligosaccharide metal coordination has been extensively studied with alkali salts, alkaline earths and even transition metals [35].

It has been previously shown that the ionic complexes are likely to be composed of several isostructures (metals coordinated to different binding sites) [36]. Consequently, each corresponding ion signal in the MS spectrum is formed from a number of subpopulations of oligosaccharides with the metal attached to different positions. The abundance of each isostructure in the whole ionic complex population will depend on the affinities of the different parts of the molecule for the dopant metal.

Although the exact proportion of each isostructure for ionic complexes is unknown, it has been shown that branched structures have a greater affinity for the alkali metal ion than linear structures [37]. As a consequence, after the IRMPD of molecules with branch and linear moieties, product ions corresponding to branched fragments are expected to have higher abundances compared to those coming from linear structures. Therefore, compounds such as LNFP II and LNFP III with branched non-reducing ends and linear reducing ends should favor ions from the non-reducing ends versus to the reducing ends as opposed to structures such as LNFP I where both reducing and non-reducing ends are linear.

We tested the above hypothesis by examining the IRMPD product ion abundances of the LNFP isomers varying the irradiation time. The product ion  $m/z$  365 corresponds to the disaccharide at the reducing end Gal (1–4)Glu coordinated to sodium and is present in the fragmentation spectra of all the LNFP isomers. Fragment  $m/z$  388 corresponds to the disaccharide at the non-reducing end Gal (1–4)GluNac in LNFP III or Gal (1–3)GluNac in LNFP I, LNFP II and LNFP V. The relative abundances of these two product ions should differ depending on the structural nature of the termini. Figure 3 shows the ratio of the abundances of the product ions  $m/z$  365 and  $m/z$  388 for each isomer versus the overall degree of fragmentation which was monitored using the loss of fucose from the precursor ion, ratio ( $m/z$ ) 730/876, as a reference.

For all the isomers, the ratio ( $m/z$ ) 365/388 reaches an asymptotic value at prolonged irradiation times. For isomers with branched non-reducing end such as LNFP II and LNFP III that ratio reaches a value of 0.1, whereas for the linear isomer LNFP I it reaches 0.25. In LNFP V the position of the fucose generates a branched-like structure at the reducing end (Scheme 1) and the ratio is in this case 0.7, as would be expected if the coordination of the sodium favors the fragment ion corresponding to the reducing end  $m/z$  365.

The influence of the position of branched moieties in the ratio ( $m/z$ ) 365/388 was confirmed with the oligosaccharide LNDFH II. LNDFH II presents both, a branched structure at the non-reducing end similar to LNFP II or LNFP III and the fucose in position Fuc (1–3)Glu at the reducing end as in isomer LNFP V (Scheme 1). The ratio in this case is constant at 0.35, which is a value approximately between the ratios obtained for LNFP II or LNFP III and LNFP V.

To probe the capability of this methodology to resolve complex samples, mixtures in different proportion of LNDFH I and LNDFH II were tested. Figure 4 shows the evolution of the ratio (m/z) 365/388 versus the overall degree of fragmentation for both pure and different mixtures of isomers.

Again, for both isomers, the ratio (m/z) 365/388 reaches an asymptotic value at prolonged irradiation times. Using the values obtained for the pure isomers as reference, the mixtures were compared and excellent agreement with the estimated theoretical average was obtained (Table 1).

### 3.3 Resolving isomers by monitoring competitive fragmentation pathways

During IRMPD the isomers of LFP all yield cross ring cleavages (CRC) except for LNFP V where the fucose is directly attached to the reducing end what appears to hinder this fragmentation pathway. Product ions 816 m/z and 756 m/z are CRC fragments formed by losses of 60 mu (<sup>0,2</sup>A) and 120 mu (<sup>0,4</sup>A), respectively, from the glucose reducing end of the precursor ion. A similar set of ions are produced when the fucose dissociates concurrently corresponding to fragments 670 m/z and 610 m/z, respectively. These two processes are in competition as illustrated in Scheme 3.

The isomers that undergo the same fragmentation pathways will have different activation barriers and will yield different abundances. We monitored the loss of the fucose from the parent versus the loss of the fucose from the fragments corresponding to the CRC products. In Figure 5 the ratio of intensities of the parent to loss of fucose (m/z) 730/876 was plotted versus the similar fragmentation from the CRC product (m/z) (670+610)/(816+756). When the fragment yield is increased, accomplished by increasing the irradiation period, the ratio of the product ion to the precursor ion increases, hence the ratio (m/z) 730/876 increases. Interestingly, the ratio of the fucose loss from the CRC fragments increases in linear manner. The results for the three oligosaccharides are shown. We observe that both LNFP I and LNFP II have the same slope corresponding to 1, while LNFP III has a considerably smaller value corresponding to 0.5. Thus, LNFP II and LNFP III can be finally differentiated. The results provide some information regarding the kinetics of the associated fragmentation pathways. While fucose loss from either fragment or molecular ion appears to involve similar energetics for LNFP I and II, the same loss for LNFP III is markedly different.

The theme of monitoring fragmentation pathways by varying dissociation energies can also be applied to other product ions. Fragment m/z 388, present in all LNFP isomers, corresponds to either the internal fragments Gal-GlcNac and GlcNac-Gal. It is often accompanied by a homologous fragment containing an additional oxygen (m/z 406). Although the presence of these ions are the result of several complicated and competing pathways (Scheme 2), their relative abundances can be monitored and compared to the overall fragmentation and represented by the loss of fucose from the parent ion (m/z) 730/876. Shown in Figure 6 is the ratio of (m/z) 388/406 as function of the ratio (m/z) 730/876. The former reaches an asymptote that can be used to differentiate, LNFP II and LNFP III. This ratio is generally reproducible and can be used to determine the percentage of each in mixture. Shown in Figure 6 are mixtures of LNFP II and LNFP III with different proportions of each isomer. The value are intermediate of the pure compounds and correspond well to that expected based on the relative abundances as shown in Table 2.

## 4. Conclusion

Oligosaccharide analysis represents a considerable challenge even with the most advanced analytical tools. Analysis may require a number of tools used together to obtain

comprehensive information. Mass spectrometry provides the best combination of high sensitivity with structural analysis. Furthermore, mass spectrometry provides more than just compositional analysis. By manipulating dissociation pathways and interpreting the fragmentation pattern from a mechanistic point of view, isomer differentiation is possible. The results presented in this report show that although complete structural information cannot be obtained using tandem MS, the fragmentation pathways can be used to differentiate isomers. It is possible, that the combination of these approaches may provide new and unexpected amount information that in turn can be used to elucidate the composition of complex isomeric mixtures. The procedures described in this study appear to be quite general and may be useful to differentiate isomeric compounds. While the methods have been applied to MALDI produced ions, they should also be applicable to ions produced by other ionization techniques such as electrospray ionization.

## Acknowledgments

This manuscript is dedicated to Professor Detlef Schroeder who was a friend and colleague. A. G. wants to thank the Spanish National Research Council for the economical supply 2009 EST CSIC-1536. Funding provided by NIH (GM R01HD061923) is gratefully acknowledged.

## Abbreviations

<b>HMO</b>	Human Milk Oligosaccharide
<b>FT-ICR</b>	Fourier Transform Ion Cyclotron Resonance mass spectrometry
<b>CRC</b>	Cross-Ring Cleavage
<b>IRMPD</b>	Infrared Multiphoton Dissociation

## References

- [1]. Delzenne NM. Oligosaccharides: state of the art. *Proceedings of the Nutrition Society*. 2003; 62:177–182. [PubMed: 12749343]
- [2]. Dell A, Morris HR. Glycoprotein Structure Determination by Mass Spectrometry. *Science*. 2001; 291:2351–2356. [PubMed: 11269315]
- [3]. Yamakawa T, Nagai Y. Glycolipids at the cell surface and their biological functions. *Trends in Biochemical Sciences*. 1978; 3:128–131.
- [4]. An HJ, Lebrilla CB. Structure elucidation of native N- and O-linked glycans by tandem mass spectrometry (tutorial). *Mass Spectrom Rev*. 2011; 30:560–578. [PubMed: 21656841]
- [5]. Bode L, Jantscher-Krenn E. Structure-Function Relationships of Human Milk Oligosaccharides. *Advances in Nutrition: An International Review Journal*. 2012; 3:383S–391S.
- [6]. Helenius A. Aeby, Markus, Intracellular Functions of N-Linked Glycans. *Science*. 2001; 291:2364–2369. [PubMed: 11269317]
- [7]. Tabak LA. The role of mucin-type O-glycans in eukaryotic development. *Seminars in Cell & Developmental Biology*. 2010; 21:616–621. [PubMed: 20144722]
- [8]. Yagi Y, Yamamoto S, Kakehi K, Hayakawa T, Ohyama Y, Suzuki S. Application of partial-filling capillary electrophoresis using lectins and glycosidases for the characterization of oligosaccharides in a therapeutic antibody. *Electrophoresis*. 2011; 32:2979–2985. [PubMed: 22145163]
- [9]. Zaia J. Mass Spectrometry and the Emerging Field of Glycomics. *Chemistry & Biology*. 2008; 15:881–892. [PubMed: 18804025]
- [10]. Mo W, Sakamoto H, Nishikawa A, Kagi N, Langridge JI, Shimonishi Y, Takao T. Structural Characterization of Chemically Derivatized Oligosaccharides by Nanoflow Electrospray Ionization Mass Spectrometry. *Analytical chemistry*. 1999; 71:4100–4106. [PubMed: 10500493]

- [11]. Morelle W, Michalski J-C. Analysis of protein glycosylation by mass spectrometry. *Nat. Protocols*. 2007; 2:1585–1602.
- [12]. Laine RA, Pamidimukkala KM, French AD, Hall RW, Abbas SA, Jain RK, Matta KL. Linkage Position in Oligosaccharides by Fast Atom Bombardment Ionization, Collision-Activated Dissociation, Tandem Mass-Spectrometry and Molecular Modeling - L-Fucosylp-(Alpha-1-]3)-D-N-Acetyl-D-Glucosamylp-(Beta-1-]3)-D-Galactosylp-(Beta-1-O-Methyl), L-Fucosylp-(Alpha-1-]4)-D-N-Acetyl-D-Glucosaminyip-(Beta-1-]3)-D-Galactosylp-(Beta-1-O-Methyl), L-Fucosylp-(Alpha-1-]6)-D-N-Acetyl-D-Glucosaminyip-(Beta-1-]3)-D-Galactosylp-(Beta-1-O-Methyl)- *J Am Chem Soc*. 1988; 110:6931–6939.
- [13]. Garozzo D, Giuffrida M, Impallomeni G, Ballistreri A, Montaudo G. Determination of linkage position and identification of the reducing end in linear oligosaccharides by negative ion fast atom bombardment mass spectrometry. *Analytical chemistry*. 1990; 62:279–286.
- [14]. Domon B, Müller DR, Richter WJ. Identification of interglycosidic linkages and sugar constituents in disaccharide subunits of larger glycosides by tandem mass spectrometry. *Org Mass Spectrom*. 1989; 24:357–359.
- [15]. Ciucanu I, Kerek F. A simple and rapid method for the permethylation of carbohydrates. *Carbohydr Res*. 1984; 131:209–217.
- [16]. Nillson B, Svensson S. A new method for degradation of the protein part of glycoproteins: isolation of the carbohydrate chains of asialofetuin. *Carbohydr Res*. 1979; 72:183–190.
- [17]. Harvey DJ. Identification of protein-bound carbohydrates by mass spectrometry. *Proteomics*. 2001; 1:311–328. [PubMed: 11680878]
- [18]. Angel, A-S.; Nilsson, B. [32] Linkage positions in glycoconjugates by periodate oxidation and fast atom bombardment mass spectrometry. In: James, AM., editor. *Methods in enzymology*. Academic Press; 1990. p. 587-607.
- [19]. Boehm G, Stahl B. Oligosaccharides from milk. *J Nutr*. 2007; 137:847s–849s. [PubMed: 17311985]
- [20]. Gyorgy P, Norris RF, Rose CS. Bifidus Factor .1. A Variant of *Lactobacillus-Bifidus* Requiring a Special Growth Factor. *Arch Biochem Biophys*. 1954; 48:193–201. [PubMed: 13125589]
- [21]. Harmsen HJM, Wildeboer-Veloo ACM, Raangs GC, Wagendorp AA, Klijn N, Bindels JG, Welling GW. Analysis of intestinal flora development in breast-fed and formula-fed infants by using molecular identification and detection methods. *J Pediatr Gastr Nutr*. 2000; 30:61–67.
- [22]. Rastall RA, Rhoades J, Manderson K, Wells A, Hotchkiss AT, Gibson GR, Formentin K, Beer M. Oligosaccharide-Mediated Inhibition of the Adhesion of Pathogenic *Escherichia coli* Strains to Human Gut Epithelial Cells In Vitro. *J Food Protect*. 2008; 71:2272–2277.
- [23]. Rudloff S, Stefan C, Pohlentz G, Kunz C. Detection of ligands for selectins in the oligosaccharide fraction of human milk. *Eur J Nutr*. 2002; 41:85–92. [PubMed: 12083318]
- [24]. Rudloff S, Bode L, Kunz C, Muhly-Reinholz M, Mayer K, Seeger W. Inhibition of monocyte, lymphocyte, and neutrophil adhesion to endothelial cells by human milk oligosaccharides. *Thromb Haemostasis*. 2004; 92:1402–1410. [PubMed: 15583750]
- [25]. Sprenger N, Angeloni S, Ridet JL, Kusy N, Gao H, Crevoisier F, Guinchard S, Kochhar S, Sigrist H. Glycoprofiling with micro-arrays of glycoconjugates and lectins. *Glycobiology*. 2005; 15:31–41. [PubMed: 15342550]
- [26]. Takada A, Ohmori K, Yoneda T, Tsuyuoka K, Hasegawa A, Kiso M, Kannagi R. Contribution of Carbohydrate Antigens Sialyl Lewis A and Sialyl Lewis X to Adhesion of Human Cancer Cells to Vascular Endothelium. *Cancer Research*. 1993; 53:354–361. [PubMed: 7678075]
- [27]. Scharfman A, Degroote S, Beau J, Lamblin G, Roussel P, Mazurier J. *Pseudomonas aeruginosa* binds to neoglycoconjugates bearing mucin carbohydrate determinants and predominantly to sialyl-Lewis x conjugates. *Glycobiology*. 1999; 9:757–764. [PubMed: 10406841]
- [28]. Barton SJ, Whittaker JC. Review of factors that influence the abundance of ions produced in a tandem mass spectrometer and statistical methods for discovering these factors. *Mass Spectrom Rev*. 2009; 28:177–187. [PubMed: 18680189]
- [29]. Memboeuf A, Nasioudis A, Indelicato S, Pollre F, Drahos L.s. Size Effect on Fragmentation in Tandem Mass Spectrometry. *Analytical chemistry*. 2010; 82:2294–2302. [PubMed: 20151701]



- [30]. Barkauskas DA, An HJ, Kronewitter SR, de Leoz ML, Chew HK, de Vere White RW, Leiserowitz GS, Miyamoto S, Lebrilla CB, Rocke DM. Detecting glycan cancer biomarkers in serum samples using MALDI FT-ICR mass spectrometry data. *Bioinformatics*. 2009; 25:251–257. [PubMed: 19073586]
- [31]. Clowers BH, Dodds ED, Seipert RR, Lebrilla CB. Dual polarity accurate mass calibration for electrospray ionization and matrix-assisted laser desorption/ionization mass spectrometry using maltooligosaccharides. *Anal Biochem*. 2008; 381:205–213. [PubMed: 18655765]
- [32]. Zaia J. Mass spectrometry of oligosaccharides. *Mass Spectrom Rev*. 2004; 23:161–227. [PubMed: 14966796]
- [33]. Gaucher SP, Leary JA. Influence of metal ion and coordination geometry on the gas phase dissociation and stereochemical differentiation of N-glycosides. *International Journal of Mass Spectrometry*. 2000; 197:139–148.
- [34]. Leavell MD, Leary JA. Stabilization and linkage analysis of metal-ligated sialic acid containing oligosaccharides. *Journal of the American Society for Mass Spectrometry*. 2001; 12:528–536. [PubMed: 11349950]
- [35]. Adamson JT, Håkansson K. Electron Capture Dissociation of Oligosaccharides Ionized with Alkali, Alkaline Earth, and Transition Metals. *Analytical chemistry*. 2007; 79:2901–2910. [PubMed: 17328529]
- [36]. Cancilla MT, Wong AW, Voss LR, Lebrilla CB. Fragmentation Reactions in the Mass Spectrometry Analysis of Neutral Oligosaccharides. *Analytical chemistry*. 1999; 71:3206–3218. [PubMed: 10450162]
- [37]. Cancilla MT, Penn SG, Carroll JA, Lebrilla CB. Coordination of Alkali Metals to Oligosaccharides Dictates Fragmentation Behavior in Matrix Assisted Laser Desorption Ionization/Fourier Transform Mass Spectrometry. *J Am Chem Soc*. 1996; 118:6736–6745.

**Highlights**

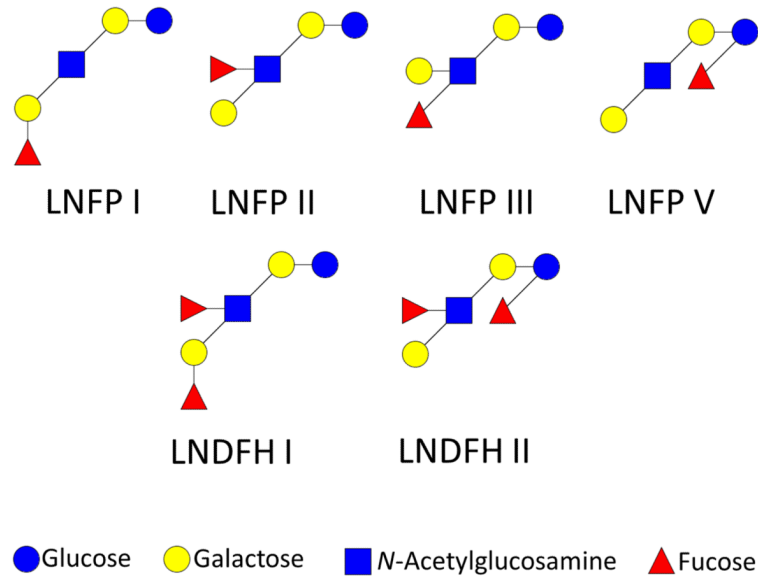
Human milk isomeric oligosaccharides were studied by MALDI FT-ICR.

IRMPD Tandem-MS experiments varying the irradiation period were performed.

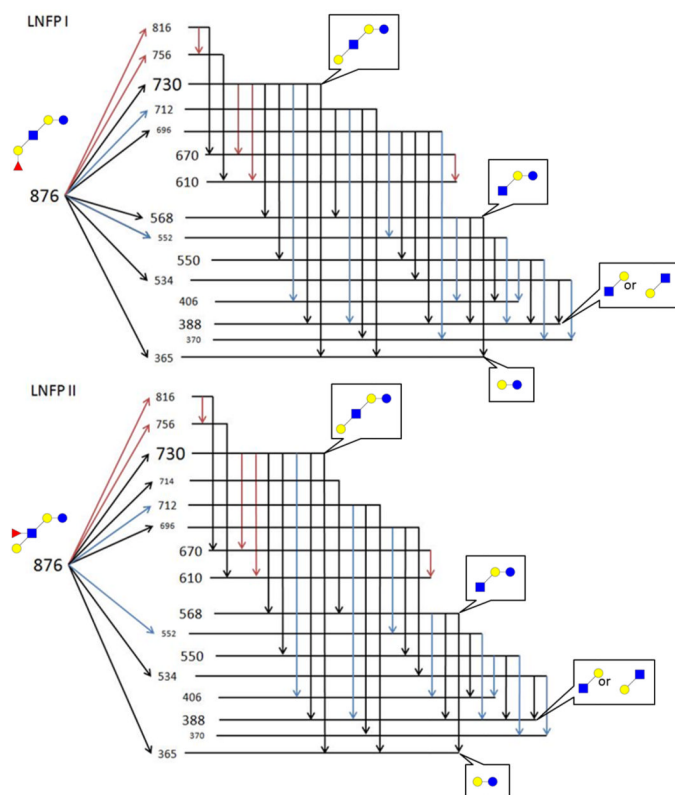
Sodium affinities and fragmentation paths were used to interpret the spectra.

Pure isomers and mixtures of these oligosaccharides were distinguished.

The rationale described can be used to resolve other isomeric species.



**Scheme 1.**  
Structure of the HMOs examined in this study.



**Scheme 2.**

Diagram of the fragmentation pathways of isomers LNFP I and LNFP II. Red arrows correspond to internal cross-ring cleavages (CRC), blue arrows correspond to the C, Z fragmentation of the glycosidic bond and black to B, Y cleavages [32]. The  $m/z$  of the species corresponds to each product ion bound to  $\text{Na}^+$ .

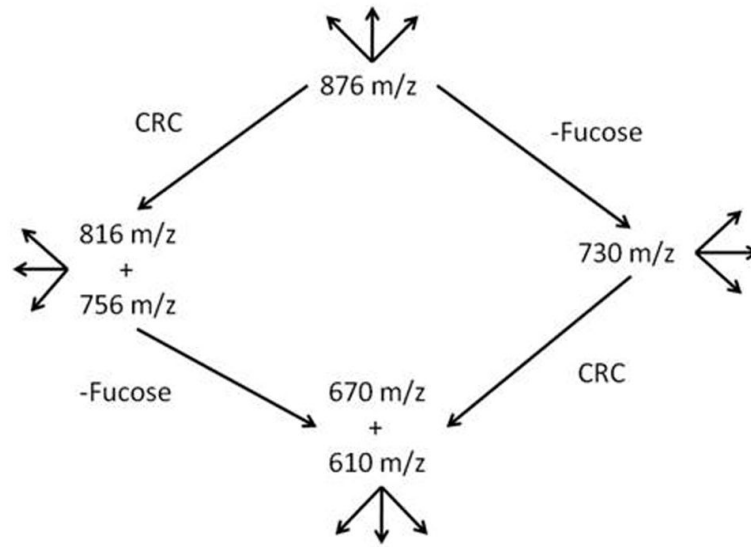
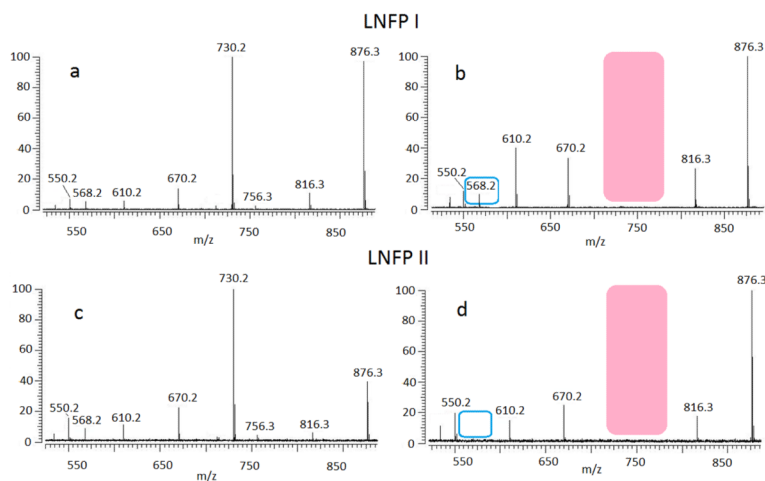
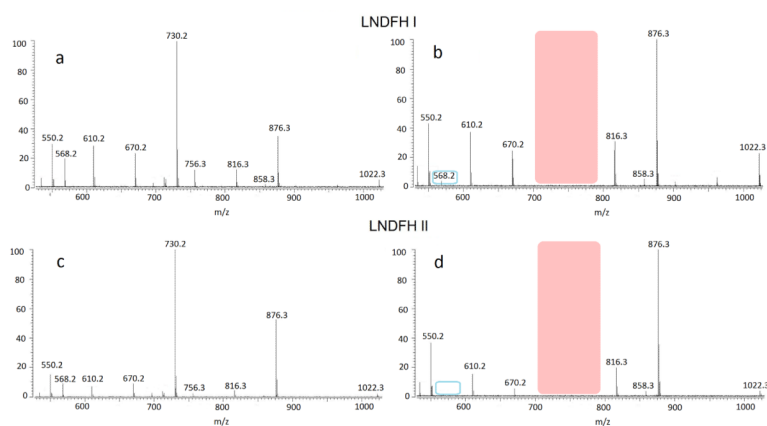
**Scheme 3.**

Diagram of the CRC vs. fucose cleavage competitive fragmentation.



**Figure 1.** IRMPD fragmentation experiments of isomers LNFP I (a, b) and LNFP II (c,d). The expulsion of species  $m/z$  730 and  $m/z$  714 during fragmentation (b, d) supposes the disappearance of product ion  $m/z$  568 only in LNFP II. The red boxes indicate the range of double resonance ejection during the IRMPD fragmentation. The blue boxes indicate the position of the potentially affected product ion.



**Figure 2.** Fragmentation experiments of isomers LNDFH I (a, b) and LNDFH II (c,d). The ejection of species  $m/z$  730 and  $m/z$  714 during IRMPD (b, d) affects the disappearance of  $m/z$  568 in LNDFH II (d). The red boxes indicate the frequency range of double resonance ejection during the IRMPD. The blue boxes indicate the position of the potentially affected product ion.

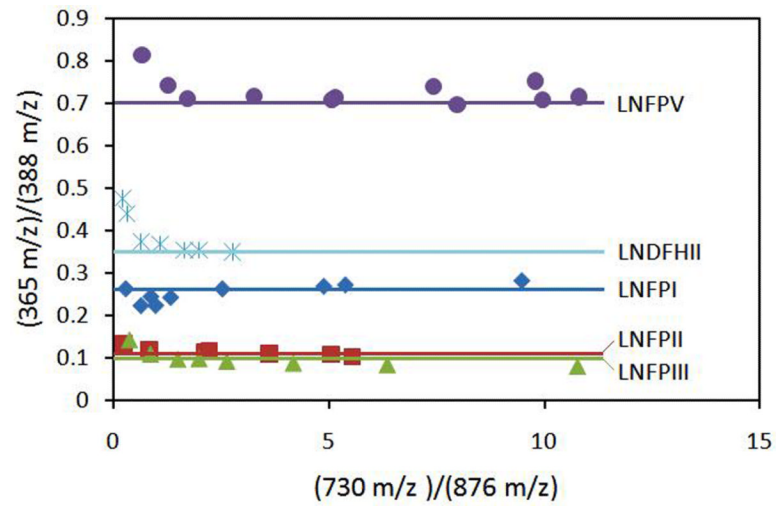


**Figure 3.** Evolution of the quotient (m/z) 365/388 during IRMPD for isomers LNFP I, LNFP II, LNFP III and LNFP V and oligosaccharide LNDFH II.



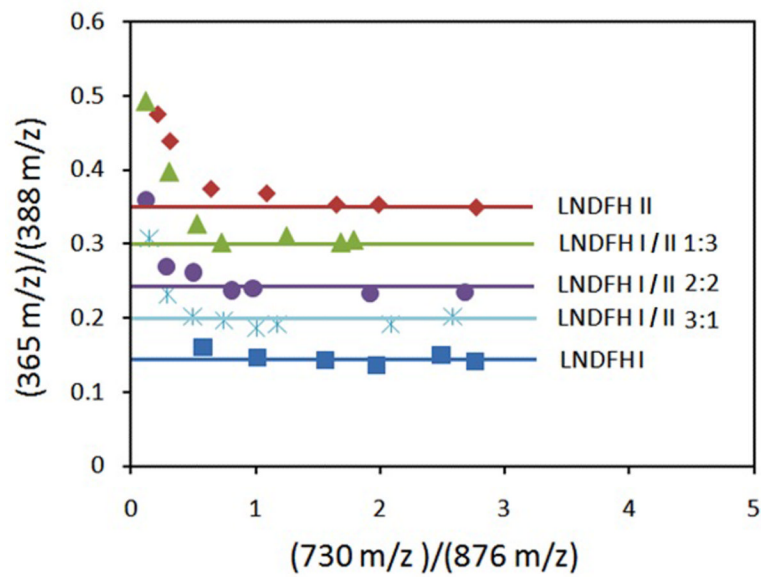


**Figure 4.** Evolution of the quotient (m/z) 365/388 during IRMPD for isomers LNDFH I, LNDFH II and mixtures in different proportion of them.

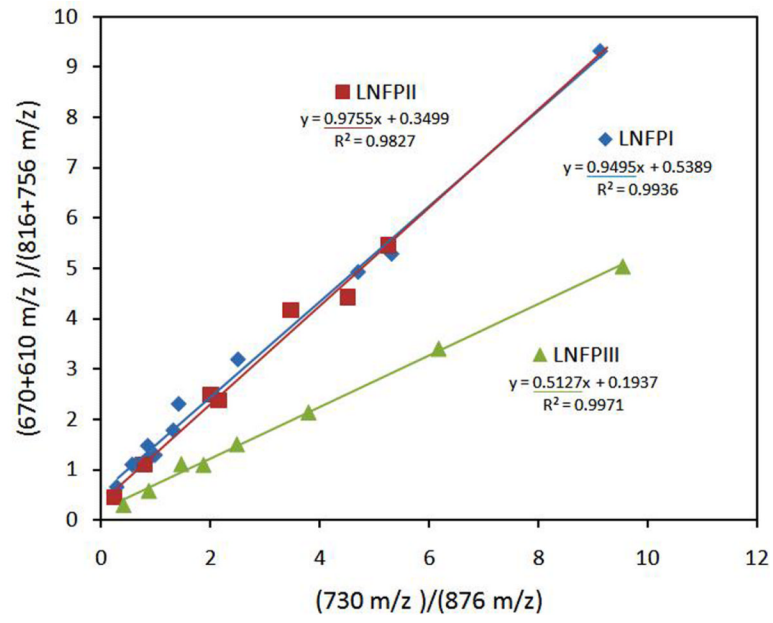


**Figure 5.**  
Evolution of CRC products during fragmentation.

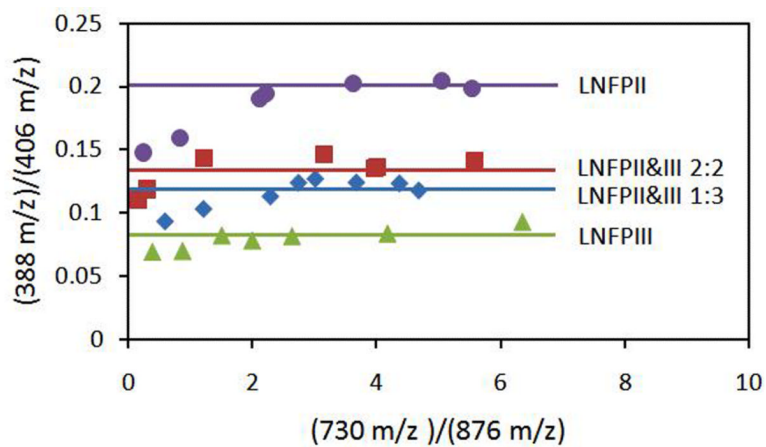


**Figure 6.** Evolution of the quotient (m/z) 388/406 during IRMPD fragmentation for isomers LNFPII, LNFPIII and mixtures in different proportion of them.

**Table 1**

Experimental<sup>a</sup> and theoretical<sup>b</sup> asymptotic values of the quotient (m/z) 365/388 for the IRMPD fragmentation of LNDFH I, LNDFH II and mixtures of them. The standard deviation of the data points used to obtain the average asymptotic value is also included.

	<b>LNDFH I</b>	<b>LNDFH II</b>	<b>LNDFH I/II 1:3</b>	<b>LNDFH I/II 2:2</b>	<b>LNDFH I/II 3:1</b>
Quotient asymptote <sup>a</sup>	0.143	0.353	0.305	0.246	0.195
Calculated average <sup>b</sup>			0.300	0.248	0.196
Standard deviation	0.005	0.002	0.004	0.015	0.007

**Table 2**

Experimental<sup>a</sup> and theoretical<sup>b</sup> asymptotic values of the quotient (m/z) 388/406 for the IRMPD fragmentation of LNFP-II, LNFP-III their mixtures. The standard deviation was determined from the asymptotic points (seven values).

	<b>LNFPII</b>	<b>LNFPIII</b>	<b>LNFPII&amp;III 1:3</b>	<b>LNFPII&amp;III 2:2</b>
Quotient asymptote <sup>a</sup>	0.198	0.084	0.119	0.141
Calculated Average <sup>b</sup>			0.112	0.141
Standard Deviation <sup>c</sup>	0.006	0.005	0.008	0.005